S. Adhikari
College of Engineering,
Swansea University,
Singleton Park,
Swansea SA2 8PP, UK

E. I. Saavedra Flores
Departamento de Ingeniería en Obras Civiles,
Universidad de Santiago de Chile,
Avenue Ecuador 3659,
Santiago, Chile

F. Scarpa
Bristol Centre for Nanoscience and
Quantum Information (NSQI),
Tyndall Avenue,
Bristol BS8 1FD, UK

R. Chowdhury
Department of Civil Engineering,
Indian Institute of Technology Roorkee,
Roorkee 247 667, India

M. I. Friswell
College of Engineering,
Swansea University,
Singleton Park,
Swansea SA2 8PP, UK

A Hybrid Atomistic Approach for the Mechanics of Deoxyribonucleic Acid Molecules

The paper proposes a new modeling approach for the prediction and analysis of the mechanical properties in deoxyribonucleic acid (DNA) molecules based on a hybrid atomistic-finite element continuum representation. The model takes into account of the complex geometry of the DNA strands, a structural mechanics representation of the atomic bonds existing in the molecules and the mass distribution of the atoms by using a lumped parameter model. A 13-base-pair DNA model is used to illustrate the proposed approach. The properties of the equivalent bond elements used to represent the DNA model have been derived. The natural frequencies, vibration mode shapes, and equivalent continuum mechanical properties of the DNA strand are obtained. The results from our model compare well with a high-fidelity molecular mechanics simulation and existing MD and experimental data from open literature. [DOI: 10.1115/1.4027690]

1 Introduction

The importance of the DNA molecule in understanding biological processes has been well established. Although DNA is symbolized by the classical double helix structure, it often exists in conjunction with other molecules in order to perform its various roles such as replication and repair [1]. The interactions of DNA with other molecules make it undergo deformations such as bending, stretching, twisting, folding, and even knotting [2]. DNA is a highly flexible structure and has the ability to withstand significant deformations without being damaged [3]. The study on the deformation of DNA is vital to understand its role in the interaction with protein molecules [1]. DNA can also be extremely useful as a basic building block for a range of atomistic scale structures [4] and is likely to play a crucial part in future generations of synthetic materials [5]. More recently, it has been shown that DNA can be used as an electronic data storage device [6]. However, to develop computing devices using DNA, it is necessary to know structural deformation and stability properties [7] under a wide range of mechanical and thermal conditions. In more general terms, it is important to understand the DNA mechanical behavior under different loading conditions for its successful use within the context of material science. Over the past two decades, it has been possible to conduct single molecule experiments and observe deformation patterns under various loading conditions [3,8–10]. It is not, however, always possible to conduct experiments in a reliable and efficient manner with DNA molecules, and the detailed configuration of DNA strands is often not completely known, especially for the case of DNA-based materials. Computational methods have been therefore developed for the mechanical analysis of DNA [11–13] and other biological molecules. The two main categories of computational methods applied to DNA molecules are classical molecular dynamics [14] and continuum mechanics [15–17]. MD is successful in capturing complex deformation mechanisms in atomistic systems, but suffers from the drawback of excessive computing costs and therefore its use has been limited to the analysis of small to moderate size problems [18]. Multiscale methods based on MD on long DNA segments have been also used [19], however at specific computational cost. Continuum models are based on the development of constitutive equations with their boundary conditions, and the estimation of the parameters defining the equivalent continuum in statics, dynamics, and stability (buckling) analysis [7,11]. Often the continuum parameters are calibrated from target experiments [20]. Finite element (FE) techniques with continuum representations of DNA strands have been applied to predict the behavior under torsional stress [16], and also for more general protein structures [12,17]. The interested Reader can find a comprehensive review about simulation and experimental methods applied to the mechanics and structural analysis of single biomolecules in Ref. [21].

The conventional finite element method applied to continuum mechanics provides an efficient way to analyze DNA and other biological structures consisting of larger length scales (>10 nm). At a smaller length, the DNA cannot be represented as a continuum, but as a connected collection of molecules which are discrete in nature from the point of view of mechanics. The basic assumption of a continuum idealization of a discrete structure can cause this approach to fail at predicting the mechanical response of systems with topological defects and local irregularities. When small length-scale effects cannot be neglected, the applicability of continuum mechanics based models may become questionable [22] no matter what solution technique is used. To deal with such discrete structures, a new generation of lattice finite element methods [23] has been proposed for homogeneous nanostructures such as carbon nanotubes [24–26] and graphene sheets [27,28]. The atomistic finite element or lattice approach [23,29] establishes a link

Manuscript received April 10, 2014; final manuscript received May 9, 2014; published online June 10, 2014. Assoc. Editor: Abraham Wang.

between the structural and molecular mechanics (MM) at the atomic bond level and provides a way to model the deformation of atomic systems by means of conventional finite element analyses using classical beam elements. In contrast to the continuum models, the lattice approach proposes a discrete representation of the system. This makes it particularly suitable for capturing local information from individual atoms and from interatomic forces, with the possibility of introducing defects or inclusions in the atomic structure. In spite of the extensive work carried out in this context, atomistic finite element simulations have been virtually restricted to the exclusive study of homogeneous structures such as carbon nanotubes and graphene sheets. In this paper, we investigate possibility of using atomistic finite element for a nonhomogeneous structure such as the DNA molecule.

In this work, we present a modeling approach based on the application of the atomistic-continuum finite element technique to DNA molecules. The model is used to derive the equivalent properties of the bonds belonging to the different chemical groups making the DNA strand. As a case study, we examine a 13-base-pair DNA model, the geometry of which is obtained from standard protein data bank (PDB) files. The model is used to identify the natural frequencies and the equivalent stiffness of the DNA strand. The rational behind the focus on the natural frequencies of DNA molecules is because of the importance of detecting its spectroscopic behavior in a wide range of applications related also to changes of states [6]. As a benchmark for the vibrational behavior identified through our model, we use a MM approach able to predict both eigenvalues and eigenmodes of the DNA strand having the same geometry of the atomistic-continuum model. Our approach compares well with the MM simulations, and experimental and MD data obtained from open literature. Moreover, it reveals how the different chemical groups of the DNA molecule behave from a mechanical point of view, and the different stiffness and structure distributions they create to obtain the equivalent continuum mechanical properties of the DNA molecule.

2 DNA Structure Mechanical Models

2.1 Finite Element Atomistic-Continuum Approach. We give here a very brief overview of the DNA structure to clarify the structural mechanics considerations needed in developing our atomistic-continuum approach. DNA is a long chain of four different small compounds called nucleotides (guanine, adenine, thymine, and cytosine), often symbolized by the letters G, A, T, and C. Each nucleotide in turn is composed by a sugar (deoxyribose) and a phosphate group. Generally, DNA molecules are double-stranded helices, consisting of two long polymers of these nucleotides. The two strands run in opposite directions to each other, one backbone being 3′ (three prime) and the other being 5′ (five prime). DNA bases pair up with each other, A with T and C with G, to form units called base pairs. From these discussions, it is evident that a homogeneous continuum mechanics model is not suitable to represent these details. One complete turn is 3.4 nm in length and has 10 base pairs. This implies that the base pairs are approximately 0.34 nm or 3.4 Å apart. The average diameter of the DNA molecule is about 2 nm. For the structural analysis of DNA, it is essential to precisely define the number of base pairs. In this work, we consider a DNA segment with 13 base pairs, as shown in Fig. 1(*a*). This particular size is selected for illustration only. The finite element method developed here is also applicable to DNA structures with a larger number base pairs.

We establish an equivalence between the interatomic energies and their mechanical counterparts by means of a lattice representation. This approach was originally proposed by Ref. [23], but restricted to the study of carbon nanotubes. In this context, the covalent bond between two atoms is assumed to behave as a three-dimensional Timoshenko beam element of circular cross section. To calculate the bond stretching force constant for covalent bonds, we adopt the expression provided by the universal force field (UFF) [30]

$$k_r = 664.12 \cdot z_i \cdot z_j / l \tag{1}$$

and is expressed in units of kcal/mol · Å^2. The parameters z_i and z_j are effective atomic charges in electron units and can be obtained from the same reference. The length l is given by the natural bond length between the pair of atoms i and j and is assumed to be the sum of atom type specific single bond radii, plus a bond order correction, plus an electronegativity correction, in accordance with Ref. [30]. Regarding the angle bend force constant, it is assumed to be a constant for all the covalent bonds, equal to $k_\theta = 100$ kcal/mol · rad^2 [31]. The torsional force constant is calculated from the corresponding torsional atomic energy, which can be defined as [31]

$$E_\tau = \frac{1}{2} v_\tau \{1 - \cos[n(\tau - \tau_o)]\} \tag{2}$$

where v_τ is the potential barrier, n the periodicity of the potential, and τ_o and τ are the reference torsion angle and actual torsion angle, respectively. If we express the angle τ as the sum between τ_o and an increment of angle, $\Delta\tau$, it is straightforward to show that Eq. (2) reduces to

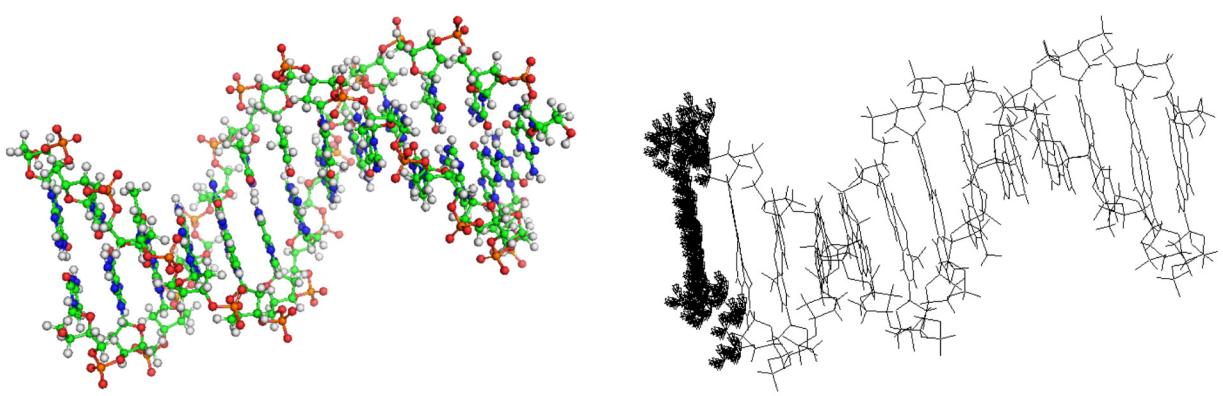

Fig. 1 The original DNA molecule from the pdb file and the converted finite element model. The nodes on the left with darker marks represent the atoms of the DNA strand which are fixed.

$$E_\tau = \frac{1}{4} v_\tau n^2 \Delta\tau^2 \tag{3}$$

when an infinitesimal increment $\Delta\tau$ is considered. By taking the second derivative of E_τ with respect to $\Delta\tau$, we can obtain the torsional force constant as

$$k_\tau = \frac{1}{2} v_\tau \cdot n^2 \tag{4}$$

with the values of v_τ and n obtained from Ref. [30]. To describe the hydrogen bonds present in the molecule, we choose the Morse potential that takes the form of

$$E_\delta = v_\delta (1 - e^{-\alpha(\delta - \delta_o)}) \tag{5}$$

The parameters v_δ and α are the depth and the inverse width of the potential describing the interaction. The parameters δ_o and δ represent the distance between atoms at equilibrium and at the deformed configuration, respectively. Finally, after taking the second derivative of the above expression with respect to the increment $\Delta\delta = \delta - \delta_o$, the stretching force constant for the hydrogen bond can be computed as

$$k_\delta = 2 v_\delta \alpha^2 \tag{6}$$

Values of v_δ and α are taken from Ref. [32], and are equal to 0.07 eV and 1.2 Å^{-1}, respectively, for all of the hydrogen bonds.

The chemical bonds of the DNA chains are represented using structural beam elements using an approach adopted in Ref. [33] for C-C sp^2, [29] for C-C sp^3, and [34] for boron nitride bonds. The three primary deformation mechanisms of an atomic bond, namely, stretching, bending, and torsion, are shown in Fig. 2. Reference [23] recognized for the first time that harmonic potentials related to stretching, in-plane bending, dihedral angle, and out-of-plane torsion have a mathematical and physical equivalence with the axial, bending, and torsional strain energies of structural beams. The mechanical properties of the bonds are calculated from the equivalence between the harmonic potentials describing the stoichiometric chemical energy and the mechanical strain energy of structural beams with deep shear deformation and circular cross section

$$\begin{aligned} \frac{k_r}{2}(\delta r)^2 &= \frac{E_b A}{2L}(\delta r)^2 \\ \frac{k_\tau}{2}(\delta\varphi)^2 &= \frac{G_b J}{2L}(\delta\varphi)^2 \quad \text{and} \\ \frac{k_\theta}{2}(\delta\theta)^2 &= \frac{E_b I}{2L}\frac{4+\Phi}{1+\Phi}(\delta\theta)^2 \end{aligned} \tag{7}$$

In Eq. (7), L is the length of the bond, while E_bA, G_bJ, and E_bI are, respectively, the equivalent axial, torsional, and bending stiffness of the bond itself. During small elastic deformations, the DNA individual bonds undergo out-of-plane torsional ($\delta\varphi$) and in-plane bending ($\delta\theta$) infinitesimal rotations, as well as small axial deformations (δr). The harmonic chemical potential is described using the force constants k_r, k_τ, k_θ, corresponding to stretching, torsional, and bending/hinging interactions. The deep shear beam correction to account for possible small aspect ratio between nominal cross section and length of the bonds is provided by the shear parameter $\Phi = 12EI/GA_sL^2$, where $A_s = A/F_s$ is the reduced cross section of the beam by the shear correction term $F_s = (6 + 12\nu + 6\nu^2)/(7 + 12\nu + 4\nu^2)$ [35]. Solving Eq. (7) and considering the formulations of the shear parameter Φ and correction term F_s leads to the solution of a nonlinear equation linking the thickness d of the beam and the Poisson's ratio ν of the equivalent material of the bond

$$k_\theta = \frac{k_r d^2}{16}\frac{4A + B}{A + B} \tag{8}$$

where

$$A = 112L^2 k_\tau + 192L^2 k_\tau \nu + 64L^2 k_\tau \nu^2 \tag{9}$$

and

$$B = 9k_r d^2 + 18k_r d^4 \nu + 9k_r d^4 \nu^2 \tag{10}$$

If we assume that the equivalent material of the bonds is transverse isotropic, one can find a unique set of thickness d and Poisson's ratio ν parameters by imposing the further constraint $G_b = E_b/2/(1 + \nu)$. Once the equivalent mechanical properties and thickness of each bond have been calculated, the DNA blocks are described following classical finite element approaches as 3D 2-node Timoshenko (deep shear) elements. Each node represents an atom which has 6 degrees of freedom (3 translational and 3

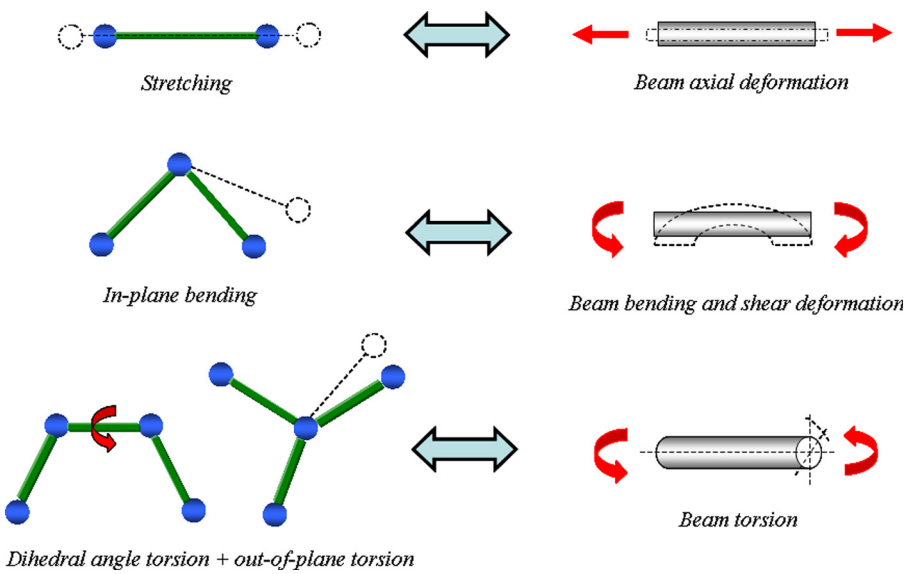

Fig. 2 The three primary deformations mechanisms of the atomic bonds

rotational). The bond elements possess a stiffness matrix $[\mathbf{K}]_e$ and a lumped parameter mass matrix $[\mathbf{M}]_e$

$$\mathbf{M}_e = \begin{bmatrix} \mathbf{M}_l & \mathbf{0} \\ \mathbf{0} & \mathbf{M}_l \end{bmatrix} \tag{11}$$

Here $[\mathbf{M}]_l = \text{diag}[m/3 \quad m/3 \quad m/3 \quad 0 \quad 0 \quad 0]^{\mathrm{T}}$, m being the mass of each atom and the rotary inertia has been neglected [29,33]. Each beam finite element is also subjected to a nodal force vector $\{\mathbf{F}\}_e$. The overall static deformation of the DNA chain can be evaluated solving the linear static equation $\{\mathbf{F}\} = \sum_e \{\mathbf{F}\}_e = \sum_e [\mathbf{K}]_e$, i.e., assembling the DNA groups according to the geometry of the chain and using a conjugate gradient method to solve the systems of equations. The natural frequencies (ω_j) and associated mode shapes $(\mathbf{x}_j)$ of the DNA structure are evaluated by solving the eigenvalue problem $([\mathbf{K}] - \omega_j^2[\mathbf{M}])\{\mathbf{x}_j\} = \{\mathbf{0}\}$, for $j = 1, 2, \ldots$. Here, $[\mathbf{K}] = \sum_e [\mathbf{K}]_e$ and $[\mathbf{M}] = \sum_e [\mathbf{M}]_e$ are the global stiffness and mass matrices after applying the boundary conditions. A Lanczos algorithm is used to compute the eigenvalues and eigenvectors of the problem. In order to carry out our numerical simulations, we adopt the commercial finite element software [36]. The geometric configuration and nodal connectivities of the DNA strand used in this work are obtained from a PDB file. The finite element mesh comprises 822 nodes that represent the atoms of the molecule. The atomic mass is modeled by means of 3D discrete mass elements lumped at each node and assigned according to the type of atom represented. The covalent bonds are modeled by means of 885 3D elastic beam elements with 3 rotational and 3 translational degrees of freedom. Transverse shear strains (Timoshenko beam theory) and Hermite interpolation are considered in the beam element formulation. When compared to the covalent bonds, the effects of van der Waals interactions are much weaker [37] and, therefore, are not considered in this work. Hydrogen bonds (which are stronger interactions) are incorporated in the model by means of 34 elastic spar elements. Zero prescribed displacements are imposed as boundary conditions on all of the degrees of freedom of the nodes located on the left side of the structure (see Fig. 1(*b*)).

2.2 Molecular Mechanics. Molecular mechanics simulations have been performed with Gaussian [38] using UFF [30]. Since force-fields use an explicit expression for the potential energy surface of a molecule as a function of the atomic coordinates, force field-based simulations are convenient. The UFF is well suited for dynamics simulations because it allows more accurate vibration simulation than many other force fields, which do not distinguish bond strengths. The UFF is a purely harmonic force field with a potential-energy expression of the form

$$E = \sum E_R + \sum E_\theta + \sum E_\phi + \sum E_\omega + \sum E_{\text{VDW}} + \sum E_{\text{el}} \tag{12}$$

The valence interactions consist of bond stretching (E_R), which is a harmonic term and angular distortions. The angular distortions are bond angle bending (E_θ), described by a three-term Fourier cosine expansion, dihedral angle torsion (E_ϕ), and inversion terms (out-of-plane bending) (E_ω). E_ϕ and E_ω are described by cosine-Fourier expansion terms. The nonbonded interactions consist of van der Waals (E_{VDW}) and electrostatic (E_{el}) terms. E_{VDW} are described by a Lennard–Jones potential and E_{el} described by a Coulombic term. The functional form of these energy terms is given as follows:

$$E_R = k_1(r - r_0)^2, \quad E_\theta = k_2(C_0 + C_1\cos\theta + C_2\cos 2\theta),$$
$$C_2 = \frac{1}{4\sin^2\theta}, \quad C_1 = -4C_2\cos\theta_0, \quad C_0 = C_2(2\cos^2\theta_0 + 1),$$
$$E_\phi = k_3(1 \pm \cos n\phi), \quad E_\omega = k_4(1 \pm \cos(n\chi - \chi_0)),$$
$$E_{\text{VDW}} = D\left[\left(\frac{r^*}{r}\right)^{12} - 2\left(\frac{r^*}{r}\right)^{6}\right] E_{\text{el}} = \frac{q_i q_j}{\varepsilon r_{ij}} \tag{13}$$

Here, k_1, k_2, k_3, and k_4 are force constants, θ_0 is the natural bond angle, D is the van der Waals well depth, r^* is the van der Waals length, q_i is the net charge of an atom, ε is the dielectric constant, and r_{ij} is the distance between two atoms. The E_{el} term is a Coulombic term and is not zero for the present case. The Gaussian program assigned the atomic charges automatically based on the atom types. The atomic charges are assigned according to "Qeq algorithm" presented by Ref. [39]. The torsion term, E_ϕ, turns out to be of great importance. Detailed values of these parameters in Eq. (13) can be found in Ref. [30]. The calculation of the frequencies and their validation for CNTs has been detailed by Ref. [40].

3 Results and Discussions

Figure 3 shows the distribution of thickness versus length for the equivalent beams representing different chemical groups within the DNA molecule after applying the energy equivalence (7). The larger variation in thickness is exhibited by the CO and CC groups, with values ranging between 0.68 Å and 1.32 Å. These values compare well with the ones related to analogous chemical groups in the open literature. CC sp^2 bonds in graphene and carbon nanotubes with equilibrium lengths of 1.42 Å have been identified having equivalent thickness values between 0.57 Å [41], 1 Å [42], and 1.13–1.37 Å [29,43]. CN groups tend to have thickness ranges confined between 0.7 Å and 1.16 Å. Strong clustering is observed for HN groups at 0.8 Å, and CH groups.

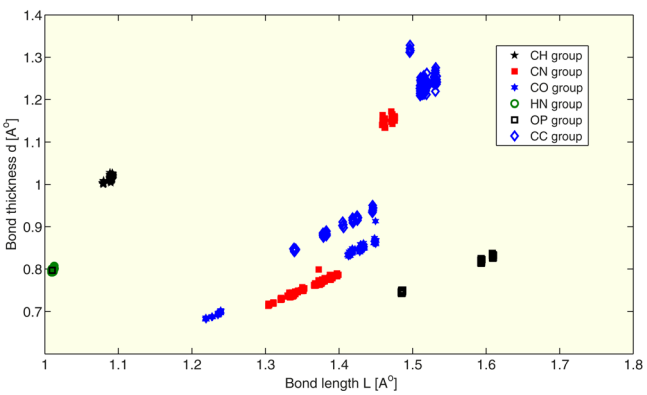

Fig. 3 The distribution of thickness versus length of equivalent beams representing different chemical groups within the DNA molecule

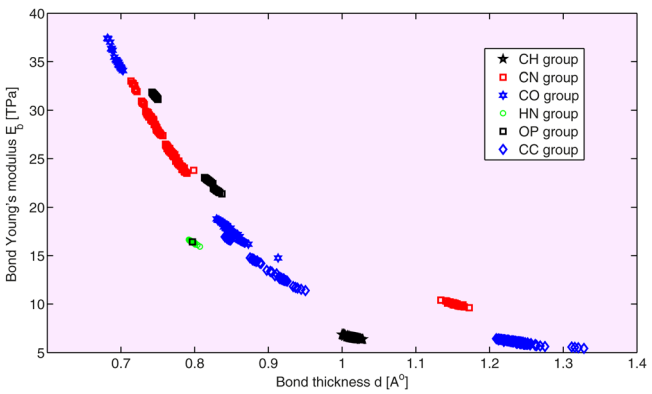

Fig. 4 The variation of Young's modulus versus thickness of equivalent beams representing different chemical groups within the DNA molecule

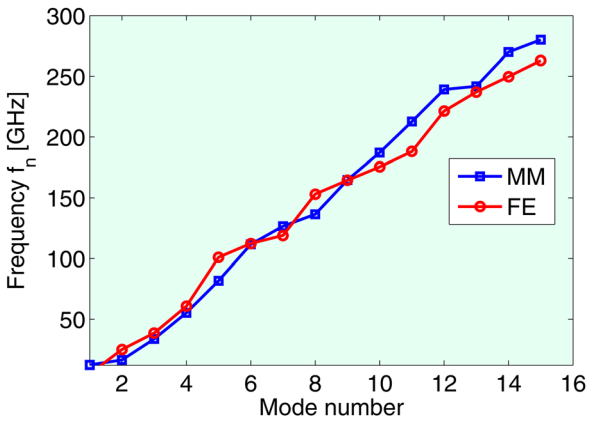

Fig. 5 Comparison between the first 15 natural frequencies obtained from the MM model and the present FE approach

The distribution of the equivalent Young's moduli (E_b) versus thickness for the different chemical groups is shown in Fig. 4. It is possible to observe a dependency with d^{-2} for the Young's moduli. This behavior can be justified assuming that a significant part of the deformation of the bonds is attributed to stretching. For a specific axial deformation and length of the bond, a relation $E_b = k_r/A = 4k_r/d^2$ can be extracted from the first of Eq. (7), therefore justifying the overall modulus/thickness trend observed. The highest Young's moduli are recorded for CO groups (33–37 TPa for $d \approx 0.7$Å). CN groups tend to exhibit tensile moduli between 23 TPa and 33 TPa for $0.7\text{Å} < d < 0.8\text{Å}$. CC groups show the lowest Young's moduli, ranging between 5 TPa and 15 TPa for $0.82\text{Å} < d < 1.34\text{Å}$. Values of 16 TPa for $d = 0.89$ Å and length of 1.42 Å have been observed in sp^2 CC bonds [33], and in BN bonds using the UFF force model for $d = 1.06$ Å and length of 1.45 Å [34]. The axially softer chemical groups appear to belong to the CC and CH phases, with some CN groups having equivalent thickness between 1.1 Å and 1.2 Å. The stiffer response is provided by CO, OP, and CN groups, the latter when the equivalent thickness is between 0.7 Å and 0.8 Å.

A direct comparison between the first 15 normal modes from the atomistic-continuum and MM model is presented in Fig. 5. One can notice a general good agreement between the two approaches. For the lower modes, the frequency obtained from the FE analysis is slightly higher than those obtained from MM (~5% for the first four modes). From mode 10 onward this trend is reversed, while the percentage error difference between the two methods oscillates between 4% and 10%. The first four mode shapes are plotted in Fig. 6. We observe that the first and second modes are associated with a global bending deformation mechanism, and the third and fourth dominated by axial deformation (springlike type behavior). The existence of bending modes associated to the first two eigenvalues is compatible with the dynamic behavior of short slenderness beams (<4) representing the whole DNA structure [44]. We note that higher modes show localized deformations, again compatible with higher frequency eigenmodes associated to structures with high modal density and complex geometry [45].

Several authors have estimated the equivalent Young's modulus for the DNA molecule assuming that the DNA strand can be

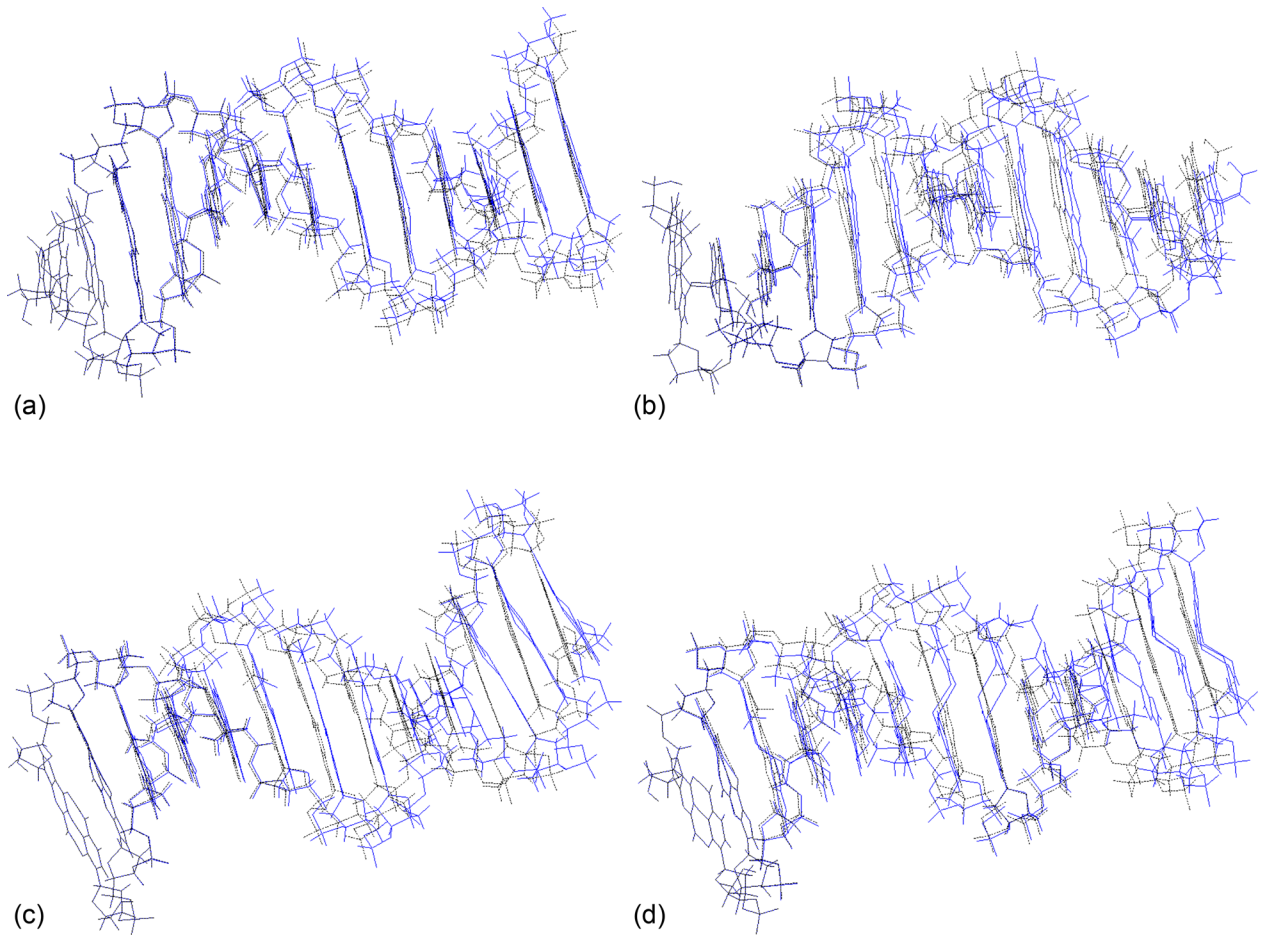

Fig. 6 The first four mode shapes for the DNA obtained from our FE model, with their corresponding natural frequencies. One side of the molecule is clamped and another side is free.

Table 1 Summary of the values published for the Young's modulus of the DNA and our numerical results

Value (MPa)	References	Comments
346 ± 30	[46]	
207 ± 37	[47]	Estimated from a force plateau of 70 pN
178 ± 31	[47]	Estimated from a force plateau of 100 pN
300–1000	[48]	
382–955	[50]	Estimated from the stretch modulus
320–789	Present FE model	

modeled as an elastic solid rod under axial stretching made from isotropic material [46–48]. The DNA structure considered in this work is not uniform along the axis of the helix. At this length-scale, the detailed geometry is far more complex than that of a homogeneous solid rod. Nevertheless, we can calculate the equivalent Young's modulus directly from the natural frequencies obtained from the eigenvalue analysis, considering the equivalent rod being fixed at one end, and free at the opposite. We consider the natural frequencies associated with a dominant mechanism of axial deformation, since the equivalent Young's modulus is related to a pure tensile-compressive load. When choosing the third and fourth frequencies ($f_3 = 38.67$ GHz and $f_4 = 60.73$ GHz), we then obtain the axial stiffness values k_i through the standard expression $k_i = M_e(2\pi f_i)^2$, with $i = 3, 4$. The equivalent stiffness of a rod with circular cross section, fixed at one edge and undergoing axial motion, is given by $k_i = E_i A/l$, where A is the cross-sectional area given by $A = \pi r^2$. Here, M_e is the effective mass of the molecule, equal to 4.3665×10^{-8}TPaÅ/GHz^2. This is one third of the mass of the whole molecule, which can be established by energy principles [49]. If we assume a uniform radius r of 10 Å for the molecule [47], with a length l of 39 Å (length of the FE model), it is straightforward to show that the Young's moduli take the values $E_3 = 320.04$ MPa and $E_4 = 789.33$ MPa, for f_3 and f_4, respectively, when the classic relation $E_i = k_i \cdot l/\pi r^2$ is adopted. Table 1 shows a comparison between our results and those values reported in the literature, demonstrating the predictive capabilities of our FE model.

The results obtained from the proposed atomistic FE method are well within the range of published results. However, the values of equivalent Young's modulus should be viewed carefully in relation to the length-scale of the DNA segment considered [50].

4 Conclusions

This paper proposes a new atomistic FE model that expresses the atomic bonds in DNA molecules by equivalent structural beams. Novel features of this approach include: (i) the ability to model the mechanics of the DNA complex geometry, (ii) the equivalent mechanical properties of the connecting bond elements determined from the atomic potentials of all of the bonds in the structure of the DNA, and (iii) the mass distribution, being taken into account with accuracy by using lumped masses at the nodes. The suitability of this modeling approach has been assessed successfully, particularly for the prediction of the equivalent Young's modulus and in calculation of the natural frequencies. The results for a thirteen base-pair DNA segment have been compared with MM simulations and with published data, demonstrating the predictive capability of the present model. This approach is computationally more efficient compared to the classical molecular dynamic simulation and compared to the continuum mechanics theory, it has the ability to incorporate atomistic details. Moreover, it can be used to perform structural mechanics predictions in DNA strands having length higher than few nanometers, bridging therefore a computational gap existing between high-fidelity molecular methods and continuum models. The results from our simulations show that the bonds of the chemical groups making the DNA molecule have different stiffness behavior, and therefore influence the dynamics of the DNA strands oscillators. CH and ON groups offer higher rigidity than analogous sp^2 C–C bonds existing in nanotubes and graphene.

We specifically considered a DNA model in this paper. The underlying modeling and computational paradigm is general and can be applied to any molecule consisting of a finite number of atomic bonds. Once the model is transformed into the finite element framework, well established numerical methods for structural analysis can be applied to analyze complex biological structures in a way that is familiar to practitioners of solid mechanics. The modeling approach can be adapted also to study highly nonlinear mechanical loading of DNA and other protein molecules, within the context of large deformations. The modeling techniques are also susceptible of being implemented in highly parallel codes to consider macroscale biological molecules.

Acknowledgment

S. Adhikari acknowledges the financial support from the Royal Society of London through the Wolfson Research Merit Award. E. I. Saavedra Flores and M. I. Friswell acknowledge the financial support from the European Research Council under the European Union's Seventh Framework Programme (FP/2007-2013)/ERC Grant Agreement No. [247045]. E. I. Saavedra Flores also acknowledges the support from the Department of Civil Engineering, University of Santiago, Chile, and also from the National Commission for Scientific and Technological Research (CONICYT), from the Chilean government. F. Scarpa acknowledges also the contribution for the CPU time from the European Union Seventh Framework Programme FP7-NMP-2009-LARGE-3MRECT.

References

[1] Balaeff, A., Koudella, C. R., Mahadevan, L., and Schulten, K., 2004, "Modelling DNA Loops Using Continuum and Statistical Mechanics," Philos. Trans. R. Soc. London, Ser. A, **362**(1820), pp. 1355–1371.
[2] Strick, T., Allemand, J.-F., Croquette, V., and Bensimon, D., 2000, "Twisting and Stretching Single DNA Molecules," Prog. Biophys. Mol. Biol., **74**(1–2), pp. 115–140.
[3] Prévost, C., Takahashi, M., and Lavery, R., 2009, "Deforming DNA: From Physics to Biology," Eur. J. Chem. Phys. Phys. Chem., **10**(9–10), pp. 1399–1404.
[4] Seeman, N. C., 2003, "DNA in a Material World," Nature, **421**(23), pp. 427–431.
[5] Pinheiro, A. V., Han, D., Shih, W. M., and Yan, H., 2011, "Challenges and Opportunities for Structural DNA Nanotechnology," Nat. Nanotechnol., **6**, pp. 763–772.
[6] Church, G. M., Gao, Y., and Kosuri, S., 2012, "Next-Generation Digital Information Storage in DNA," Science, **337**(6102), p. 1628.
[7] Forth, S., Deufel, C., Sheinin, M., Daniels, B., Sethna, J., and Wang, M., 2008, "Abrupt Buckling Transition Observed During the Plectoneme Formation of Individual DNA Molecules," Phys. Rev. Lett., **100**(14), p. 148301.
[8] Bryant, Z., Stone, M. D., Gore, J., Smith, S. B., Cozzarelli, N. R., and Bustamante, C., 2003, "Structural Transitions and Elasticity From Torque Measurements on DNA," Nature, **424**(17), pp. 338–341.
[9] Bustamante, C., Bryant, Z., and Smith, S., 2003, "Ten Years of Tension: Single-Molecule DNA Mechanics," Nature, **421**(23), pp. 423–427.
[10] Williams, M. C., Rouzina, I., and McCauley, M. J., 2009, "Peeling Back the Mystery of DNA Overstretching," Proc. Natl. Acad. Sci. U.S.A., **106**(43), pp. 18047–18048.
[11] Chou, K., 1983, "Low-Frequency Vibrations of Helical Structures in Protein Molecules," Biochem. J., **209**, pp. 573–580.
[12] Bathe, M., 2008. "A Finite Element Framework for Computation of Protein Normal Modes and Mechanical Response," Proteins: Struct. Funct. Bioinf., **70**(4), pp. 1595–1609.
[13] Manghi, M., Destainville, N., and Palmeri, J., 2012, "Mesoscopic Models for DNA Stretching Under Force: New Results and Comparison With Experiments," Eur. Phys. J. E, **94**(110), pp. 1–13.
[14] Brickmann, J., and Schmitt, U., 1999. "Classical Molecular Dynamics Simulations With Quantum Degree of Freedom," *Molecular Dynamics: From Classical to Quantum Methods*, P. B. Balbuena and J. M. Seminario, ed., Elsevier Science B.V., Amsterdam.
[15] Balaeff, A., Mahadevan, L., and Schulten, K., 2006, "Modelling DNA Loops Using the Theory of Elasticity," Phys. Rev. Lett., **73**(031919), pp. 1–23.

[16] White, J. H., and Bauer, W. R., 2004, "Finite-Element Analysis of the Displacement of Closed DNA Loops Under Torsional Stress," Philos. Trans. R. Soc. London, Ser. A, **362**(1820), pp. 1335–1353.
[17] Ma, L., Yethiraj, A., Chen, X., and Cui, Q., 2009, "A Computational Framework for Mechanical Response of Macromolecules: Application to the Salt Concentration Dependence of DNA Bendability," Biophys. J., **96**(9), pp. 3543–3554.
[18] Buehler, M. J., 2008, *Atomistic Modeling of Materials Failure*, Springer, NY.
[19] Villa, E., Balaeff, A., and Schulten, K., 2005, "Structural Dynamics of the *lac* Repressor-DNA Complex Revealed by a Multiscale Simulation," Proc. Natl. Acad. Sci. U.S.A., **102**(19), pp. 6783–6788.
[20] van Eijck, L., Merzel, F., Rols, S., Ollivier, J., Forsyth, V. T., and Johnson, M. R., 2011, "Direct Determination of the Base-Pair Force Constant of DNA From the Acoustic Phonon Dispersion of the Double Helix," Phys. Rev. Lett., **107**, p. 088102.
[21] Lavery, R., Lebrun, A., Allemand, J.-F., Bensimon, D., and Croquette, V., 2002, "Structure and Mechanics of Single Biomolecules: Experiment and Simulation," J. Phys.: Condens. Matter, **14**(14), pp. R383–R414.
[22] Zhang, Y. Y., Wang, C. M., Duan, W. H., Xiang, Y., and Zong, Z., 2009, "Assessment of Continuum Mechanics Models in Predicting Buckling Strains of Single-Walled Carbon Nanotubes," Nanotechnology, **20**(39), p. 395707.
[23] Li, C., and Chou, T. W., 2003, "A Structural Mechanics Approach for the Analysis of Carbon Nanotubes," Int. J. Solids Struct., **40**, pp. 2487–2499.
[24] Batra, R., and Sears, A., 2007, "Continuum Models of Multi-Walled Carbon Nanotubes," Int. J. Solids Struct., **44**(22–23), pp. 7577–7596.
[25] Tserpes, K. I., and Papanikos, P., 2005, "Finite Element Modeling of Single-Walled Carbon Nanotubes," Composites Part B, **36**(5), pp. 468–477.
[26] Saavedra Flores, E. I., Adhikari, S., Friswell, M. I., and Scarpa, F., 2011, "Hyperelastic Axial Buckling of Single Wall Carbon Nanotubes," Physica E, **44**(2), pp. 525–529.
[27] Scarpa, F., Adhikari, S., and Phani, A. S., 2009, "Effective Elastic Mechanical Properties of Single Layer Graphene Sheets," Nanotechnology, **20**(6), p. 065709.
[28] Liu, X., Metcalf, T. H., Robinson, J. T., Houston, B. H., and Scarpa, F., 2012, "Shear Modulus of Monolayer Graphene Prepared by Chemical Vapor Deposition," Nano Lett., **12**(2), pp. 1013–1017.
[29] Scarpa, F., Chowdhury, R., and Adhikari, S., 2011, "Thickness and In-Plane Elasticity of Graphane," Phys. Lett. A, **375**(20), pp. 2071–2074.
[30] Rappé, A. K., Casewit, C. J., Colwell, K. S., Goddard, W. A., and Skiff, W. M., 1992, "UFF, a Full Periodic Table Force Field for Molecular Mechanics and Molecular Dynamics Simulations," J. Am. Chem. Soc., **114**(25), pp. 10024–10035.
[31] Mayo, S. L., Olafson, B. D., and Goddard III, W. A., 1990, "DREIDING: A Generic Force Field for Molecular Simulations," J. Phys. Chem., **94**(26), pp. 8897–8909.
[32] Zdravković, S., and Satarić, M. V., 2011, "Transverse Interaction in DNA Molecule," Biosystems, **105**(1), pp. 10–13.
[33] Scarpa, F., and Adhikari, S., 2008, "A Mechanical Equivalence for the Poisson's Ratio and Thickness of c–c Bonds in Single Wall Carbon Nanotubes," J. Phys. D, **41**(8), p. 085306.
[34] Boldrin, L., Scarpa, F., Chowdhury, R., and Adhikari, S., 2011, "Effective Mechanical Properties of Hexagonal Boron Nitride Nanosheets," Nanotechnology, **22**(50), p. 505702.
[35] Kaneko, T., 1974. "On Timoshenko's Correction for Shear in Vibrating Beams," J. Phys. D, **8**, p. 1927.
[36] ANSYS, 2010, *Release 13.0 Documentation*, Southpointe, Canonsburg, PA.
[37] Leung, A., Guo, X., He, X., Jiang, H., and Huang, Y., 2006, "Postbuckling of Carbon Nanotubes by Atomic-Scale Finite Element," J. Appl. Phys., **99**(12), p. 124308.
[38] Frisch, M. J., Trucks, G. W., Schlegel, H. B., Scuseria, G. E., Robb, M. A., Cheeseman, J. R., Scalmani, G., Barone, V., Mennucci, B., Petersson, G. A., Nakatsuji, H., Caricato, M., Li, X., Hratchian, H. P., Izmaylov, A. F., Bloino, J., Zheng, G., Sonnenberg, J. L., Hada, M., Ehara, M., Toyota, K., Fukuda, R., Hasegawa, J., Ishida, M., Nakajima, T., Honda, Y., Kitao, O., Nakai, H., Vreven, T., Montgomery, Jr., J. A., Peralta, J. E., Ogliaro, F., Bearpark, M., Heyd, J. J., Brothers, E., Kudin, K. N., Staroverov, V. N., Kobayashi, R., Normand, J., Raghavachari, K., Rendell, A., Burant, J. C., Iyengar, S. S., Tomasi, J., Cossi, M., Rega, N., Millam, J. M., Klene, M., Knox, J. E., Cross, J. B., Bakken, V., Adamo, C., Jaramillo, J., Gomperts, R., Stratmann, R. E., Yazyev, O., Austin, A. J., Cammi, R., Pomelli, C., Ochterski, J. W., Martin, R. L., Morokuma, K., Zakrzewski, V. G., Voth, G. A., Salvador, P., Dannenberg, J. J., Dapprich, S., Daniels, A. D., Farkas, O., Foresman, J. B., Ortiz, J. V., Cioslowski, J., and Fox, D. J., 2009, *Gaussian 09, Revision A.1*, Gaussian, Inc., Pittsburgh, PA.
[39] Rappé, A. K., and Goddard, W. A., 1991. "Charge Equilibration for Molecular-Dynamics Simulations," J. Phys. Chem., **95**(8), pp. 3358–3363.
[40] Chowdhury, R., Adhikari, S., Wang, C. Y., and Scarpa, F., 2010, "A Molecular Mechanics Approach for the Vibration of Single Walled Carbon Nanotubes," Comput. Mater. Sci., **48**(4), pp. 730–735.
[41] Huang, Y., Wu, J., and Hwang, K. C., 2006, "Thickness of Graphene and Single-Wall Carbon Nanotubes," Phys. Rev. B, **74**(24), p. 245413.
[42] Batra, R., and Gupta, S., 2008, "Wall Thickness and Radial Breathing Modes of Single-Walled Carbon Nanotubes," ASME J. Appl. Mech., **75**(6), p. 061010.
[43] Hemmasizadeh, A., Mahzoon, M., Hadi, E., and Khandan, R., 2008, "A Method for Developing the Equivalent Continuum Model of a Single Layer Graphene Sheet," Thin Solid Films, **516**(21), pp. 7636–7640.
[44] Blevins, R. D., 1979, *Formulas for Natural Frequency and Mode Shape*, Van Nostrand, NY.
[45] Lyon, R. H., and DeJong, R. G., 1995, *Theory and Application of Statistical Energy Analysis*, 2nd ed., Butterworth-Heinemann, Boston, MA.
[46] Smith, S., Cui, Y., and Bustamante, C., 1996, "Overstretching B-DNA: The Elastic Response of Individual Double-Stranded and Single-Stranded DNA Molecules," Science, **271**(5250), pp. 795–799.
[47] Morii, T., Mizuno, R., Haruta, H., and Okada, T., 2004, "An AFM Study of the Elasticity of DNA Molecules," Thin Solid Films, **464–465**, pp. 456–458.
[48] Bloom, K., 2007. "Beyond the Code: The Mechanical Properties of DNA as They Relate to Mitosis," Chromosoma, **117**(2), pp. 103–110.
[49] Inman, D. J., 2003, *Engineering Vibration*, Prentice Hall PTR, NJ.
[50] Noy, A., and Golestanian, R., 2012, "Length Scale Dependence of DNA Mechanical Properties," Phys. Rev. Lett., **109**(22), p. 228101.